RSC Advances

This is an *Accepted Manuscript*, which has been through the Royal Society of Chemistry peer review process and has been accepted for publication.

Accepted Manuscripts are published online shortly after acceptance, before technical editing, formatting and proof reading. Using this free service, authors can make their results available to the community, in citable form, before we publish the edited article. This *Accepted Manuscript* will be replaced by the edited, formatted and paginated article as soon as this is available.

You can find more information about *Accepted Manuscripts* in the Information for Authors.

Please note that technical editing may introduce minor changes to the text and/or graphics, which may alter content. The journal's standard Terms & Conditions and the Ethical guidelines still apply. In no event shall the Royal Society of Chemistry be held responsible for any errors or omissions in this *Accepted Manuscript* or any consequences arising from the use of any information it contains.

ROYAL SOCIETY OF CHEMISTRY

www.rsc.org/advances

Please do not adjust margins

Journal Name

ARTICLE

Identification of 2-subsituted Benzothiazole Derivatives as Triple-functional agents with potential for AD Therapy

Received 00th January 20xx,
Accepted 00th January 20xx

DOI: 10.1039/x0xx00000x

www.rsc.org/

Liu Jiang[a], Minkui Zhang[a], Li Tang[a], Qinjie Weng[a], Yanhong Shen[b], Yongzhou Hu[a], Rong Sheng[a]*

A novel series of 2-subsituted benzothiazole derivatives as MTDLs were designed and synthesized for AD Therapy using pharcacophore-combine strategy. The benzothiazole moiety from ThT and the HPO moiety from deferiprone were connected with vinyl linker to achieve target compounds. The biological evaluation results revealed that the majority of them demonstrated desirable triple functions by interfering with Aβ aggregation, oxidative stress and metal dyshomeostasis simultaneously. The two most attractive compounds **9c** and **9i** exhibited excellent self-$A\beta_{1-42}$ aggregation inhibitory activity, efficient $ABTS^{\bullet+}$ scavenging activity, potent biometals chelating properties, as well as disaggregation activity against previous formed $A\beta_{1-42}$ fibrils. In addition to these advantages, both of them displayed no cytotoxicity to human glioma U251 cells up to 50 μM, thereby meriting further investigation.

1 Introduction

Alzheimer's disease (AD), featuring progressive memory loss and other irreversible cognitive impairments, is the most common form of dementia that afflicts more than 24 million people worldwide[1]. Despite the tremendous efforts devoted to this serious neurodegenerative disease since its discovery more than 100 years ago, the exact etiology of AD still remains elusive[2]. So far, no therapeutic agents have been available other than several drugs approved for the symptomatic treatment of AD, including three cholinesterase (AChE) inhibitors (donepezil, rivastigmine, and galantamine) and one N-methyl-D-aspartate (NMDA) receptor antagonist (memantine)[3,4].

Numerous evidences indicate that diverse factors are responsible for the initiation and progression of this complex disease, including amyloid-β (Aβ) aggregation, τ-protein hyper-phosphorylation, oxidative stress, metal ion dyshomeostasis, decreased levels of acetylcholine, neuroinflammation in central nervous system(CNS), and so on[5-18]. Reasoning this, recently more efforts have been focused on the development of multi-target-directed-ligands (MTDLs), which interfere with two or more causes of AD simultaneously and may achieve better therapeutic efficacy through complementary mechanism[5,19].

Evidences show that the rising Aβ monomer level in the brain (resulting from unbalanced Aβ production and clearance) promotes the formation of dimers and larger oligomers, and then oligomers aggregate progressively to form protofibrils, fibrils and plaques of fibrils, the major histopathological hallmark of AD[19-21]. Aggregated Aβ species are neurotoxic, so compounds capable of inhibiting Aβ aggregation may exert potential therapeutic effect on AD[22-24]. Benzothiazole derivative Thioflavin T (ThT) is the most widely used Aβ aggregation indicator *in vitro*, which displays fluorescence enhancement and a characteristic red shift when binding to Aβ aggregates[25,26]. Recently, its analogue Flutemetamol ^{18}F has been approved by FDA as the PET tracer for imaging β-amyloid (Aβ) deposition in AD patients[27]. In addition, natural stilbene derivative resveratrol also exhibits extraordinary binding affinity to amyloid aggregates, and its analogue Florbetaben ^{18}F launched in clinic for Aβ deposits imaging[28-30]. Due to their high affinity to Aβ, benzothiazole and stilbene scaffold have been frequently incorporated into different molecules for attaining Aβ aggregation inhibitory activity.[31,32].

Meanwhile, remarkably high concentration of biometals (Cu, ~ 0.4 mM. Zn, ~ 1.0 mM. Fe, ~ 0.9 mM) was found to co-localize with the amyloid deposits in AD-affected brains. Research reveals that these biometals can rapidly facilitate Aβ aggregation through binding to three histidines (H6, H13 and H14) of Aβ peptide. Besides, the binding of iron and copper to Aβ species generates reactive oxygen species (ROS), which may result in oxidative

[a]College of Pharmaceutical Sciences, Zhejiang University, Hangzhou 310058, China
[b]College of Chemistry and Environmental Science, Anyang Institute of Technology, Anyang 455000, China.
*Corresponding authors:
Rong Sheng Tel/Fax: +86-571-8820-8458, E-mail address: shengr@zju.edu.cn.

RSC Advances Accepted Manuscript

Please do not adjust margins

damage to biological molecules[11-18]. Owing to these, blocking metals-induced Aβ aggregation and reducing oxidative stress have been regarded as a promising approach for AD therapy. During the pursuit of MTDLs, Deferiprone for iron overload in thalassemia major has attracted much attention as an oral metal chelator, in which 3-hydroxy-4-pyridinone (HPO) plays a vital role in chelating activity on copper, zinc and iron ions as well as potential radical scavenging activity. Orvig' group has reported several series of HPO derivatives as MTDLs with potential AD therapeutic effect[32-36]. Among them, **HL_5** and **HL_{12}**, incorporating both benzothiazole and HPO moieties, exhibit metal chelating activity, along with Aβ aggregation inhibitory potency[32,33]. In addition, **HL_{12}** also demonstrates potent antioxidant activity similar to Trolox. However, the relatively high cytotoxicity hinders its further development. [32]

2 Rational design of novel MTDLs

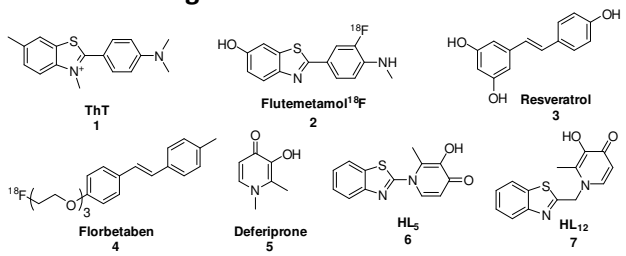

Figure 1. Structures of lead compounds

As a continuation of our previous work on 3-substituted indole and 1-phenyl-3-hydroxy-4-pyridinone derivatives as multifunctional agents for AD therapy[37,38], herein, we report a series of 2-subsituted benzothiazole derivatives (**9a-o**) as the novel multifunctional agents capable of interfering with Aβ aggregation, metal dyshomeostasis and oxidative stress simultaneously.

To develop a novel MTDLs capable of targeting the above three AD pathological factors, we undertook a rational drug design using pharmacophore-combination strategy. The benzothiazole moiety from ThT (Aβ aggregation inhibition pharmacophore) was connected with 3-hydroxy-4-pyridinone from deferiprone (metal chelating and radical scavenging pharmacophore) using a vinyl linker. The newly designed 2-benzothiazole derivatives share the similar scaffold to resveratrol, which may be beneficial to improve the binding affinity with Aβ as well as to enhance the antioxidant activity through conjugation effect. In addition, the HPO moiety was replaced by its bioisostere 3-hydroxy-4-pyranone from maltol (a wildly used food flavoring agent)[39] to ameliorate the toxic profile of compounds. To investigate the structural activity relationship (SAR) of these newly designed compounds and find optimal compounds for further development, the substituent in the benzothiazole ring was modified. The benzoxazole and N-methyl-benzoimidazole were introduced into the molecule as the bioisostere of benzothiazole. In these newly designed compounds, the benzothiazole or similar moieties and stilbene-similar scaffold may demonstrate Aβ aggregation inhibitory activity, and the 3-hydroxy-4-pyridinone (3-hydroxy-4-pyranone) moiety may exert metal chelating and anti-oxidant activity. In addition, all the structural elements of compounds were selected to adhere to the values of Lipinski's rules (Table S1).

To confirm the rationality of our design strategy, the molecular docking study of 2-substituted-benzothiazole derivative **9a** and **HL_{12}** with $Aβ_{1-42}$ (PDB ID: 1IYT) were performed using SYBYL-X 1.3 software package (Tripos, Inc.)[40].

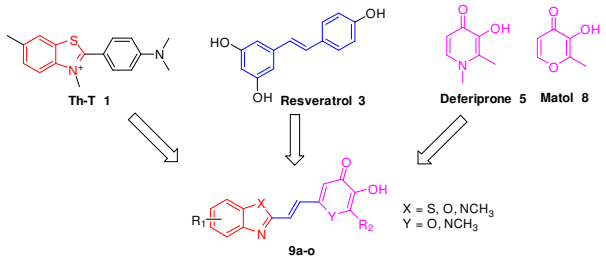

Figure 2. Rational design of 2-subsituted benzothiazole derivatives as MTDLs

As shown in Figure 3, although both **HL_{12}** and compound **9a** are located nearby the N-terminus (residues 1–17) of $Aβ_{1-42}$, they interacted with the $Aβ_{1-42}$ residues in different manners. The 3-hydroxy group of **HL_{12}** formed hydrogen bond with Lys16 at a distance of 2.84 Å, and the benzothiazole moiety interacted with His13 through another hydrogen bond (2.99 Å), which was similar to the docking result of **HL_{12}** with $Aβ_{1-40}$.[32] For compound **9a**, the oxygen of pyranone moiety formed hydrogen bond (2.42 Å) with Leu17 of $Aβ_{1-42}$. In addition, the benzothiazole moiety was embedded in a groove formed by Lys16 and Phe20 and interacted with the amino group of Lys16 at a distance of 2.96 Å. On the basis of the molecular modeling results, we considered that the compound **9a** could bind monomeric Aβ so that it was able to inhibit self-induced Aβ aggregation by disturbing the formation of β-sheets.

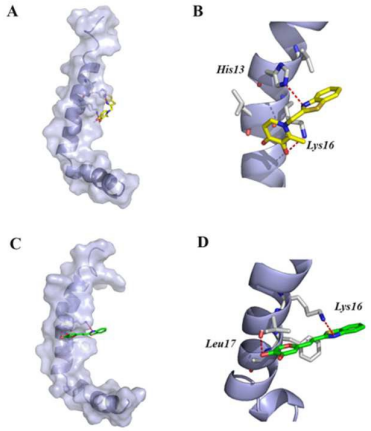

Figure 3. Docking studies of **9a** and **HL_{12}** with $Aβ_{1-42}$ (PDB code 1IYT). (A, B) Binding mode of **9a** (colored yellow) with $Aβ_{1-42}$ monomer. The hydrogen bonds between **9a** and residues Leu16 and Lys17 are indicated by red lines. (C, D) Binding mode of **HL_{12}** (colored green) with $Aβ_{1-42}$ monomer. The hydrogen bonds between HL_{12} and residues Leu17, Lys16 are indicated by red lines.

3 Results and discussion

3.1 Synthesis

The synthetic route of 2-substituted-benzothiazole derivatives **9a-o** is outlined in Scheme **1**. Protection of phenol moiety of compound **10a** and **10b** with para-methoxy benzyl chloride (PMB-

RSC Advances Accepted Manuscript

This journal is © The Royal Society of Chemistry 20xx

Cl) gave **11a** and **11b**, which were oxidized to benzaldehyde derivatives **12a** and **12b** using MnO_2, respectively. Condensation of **12a**, **b** with 2-methyl-benzothaizole (or 2-methyl-benzoxazole, or N-methyl-2-methyl-benzoimidazole) in HAc-Ac_2O under microwave condition afforded compounds **13a-h**, **13j** and **13l**, followed by deprotection of -OAc with K_2CO_3 to furnish target compounds **9a-9h**, **9j** and **9l**. Demethylatin of compounds **9g**, **9j** and **9l** with BBr_3 in CH_2Cl_2 gave 6-hydroxy derivatives **9i**, **9k** and **9m**, respectively. For the 3-hydroxy-4-pyridinone derivatives, condensation of **11a** with methylamine gained compound **14**, which was oxidized to aldehyde **15** with MnO_2. Condensation of compounds **16a**, **b** with triethyl phosphite gave compounds **17a**,**b**, which experienced Aldol condensation with aldehyde **15** to give compound **18a**, **b**. Finally, deprotection of **18a**, **b** with CF_3COOH provided target compounds **9n** and **9o**.

Scheme 1. Synthetic route to compounds **9a-9o.**

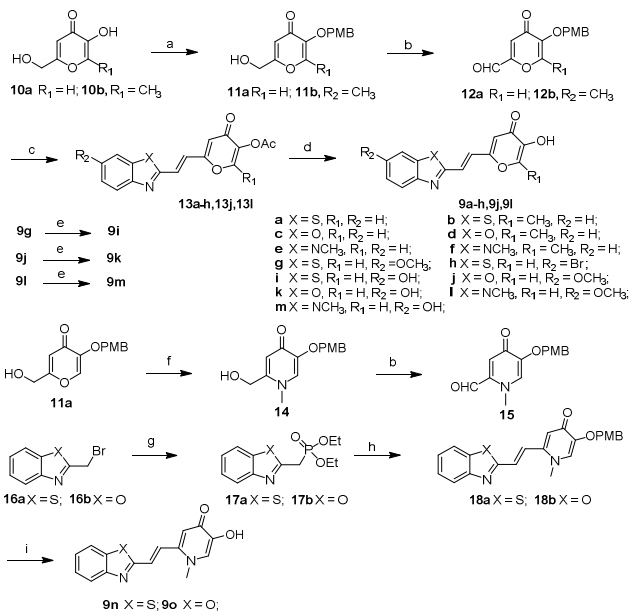

Reagents and conditions. (a) PMB-Cl, K_2CO_3, DMF, 80 °C. (b) MnO_2, $CHCl_3$, reflux. (c) 2-methyl-benzothaizole, or 2-methyl-benzoxazole, or N-methyl-2-methyl-benzoimidazole, HAc, Ac_2O, microwave. (d) K_2CO_3, MeOH, r.t. (e) BBr_3, CH_2Cl_2. (f) CH_3NH_2, H_2O, reflux. (g) $P(OEt)_3$, reflux. (h) NaH, dry THF, r.t .(i) CF_3COOH, CH_2Cl_2.

3.2 Biological evaluation

3.2.1. Inhibition of Self-Induced $A\beta_{1-42}$ Aggregation

The inhibitory ability of compounds **9a-9o** against self-induced $A\beta_{1-42}$ aggregation was measured by thioflavin T (ThT) fluorescence assay, and curcumin was used as control. Table 1 showed that all the compounds demonstrated moderate to excellent $A\beta_{1-42}$ self-aggregation inhibitory activity, and seven of them were more potent (IC_{50} values ranging from 5.06 μM to 8.25 μM) than curcumin (IC50 = 8.48 μM) and two positive controls **HL_5** (IC50 = 9.78 μM), **HL_{12}** (IC_{50} = 8.75 μM).

The primary SAR revealed that the modification of benzothiazole ring affected the activity obviously, for instance, the benzoxazole and N-Me-benzoimidazole rings were more beneficial for $A\beta_{1-42}$ aggregation inhibition than benzothiazole (such as **9c**, **9e** vs **9a**; **9d**, **9f** vs **9b**). Introduction of methyl at the C-2 position of pyranone impacted slightly on activity, such as **9a** vs **9b**; **9e** vs **9f**. The obviously increased activities of compounds **9g, 9j, 9i, 9k** (IC_{50} = 6.32, 8.25, 5.06, 5.38 μM, respectively) compared with **9a** (43.82% inhibition in 20 μM) revealed that introduction of methoxy or hydroxy moiety into the 6-position of benzothiazole was beneficial for $A\beta_{1-42}$ aggregation inhibition.

Table 1. Biological activities of compounds **9a-9o**

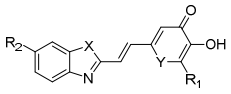

Compd.	X	Y	R_2	R_1	Inhibition of self-induced $A\beta_{1-42}$ aggregation (%) [a]	IC_{50} (μM) [d]	TEAC Values[b]
9a	S	O	H	H	43.82±5.54	n.t.[c]	4.03±0.02
9b	S	O	H	CH_3	49.36±2.01	n.t.[c]	1.45±0.09
9c	O	O	H	H	64.95±5.84	7.05±0.42	4.29±0.03
9d	O	O	H	CH_3	59.20±2.48	12.45±1.17	1.34±0.25
9e	NCH_3	O	H	H	62.35±3.42	10.36±0.67	2.31±0.21
9f	NCH_3	O	H	CH_3	71.41±1.50	9.23±1.05	1.55±0.06
9g	S	O	OCH_3	H	67.40±2.30	6.32±1.78	2.10±0.021
9h	S	O	Br	H	46.82±3.42	n.t.[c]	1.31±0.81
9i	S	O	OH	H	78.26±3.93	5.06±1.02	6.03±0.12
9j	O	O	OCH_3	H	65.12±2.53	8.25±0.41	2.69±0.32
9k	O	O	OH	H	80.42±5.36	5.38±0.57	4.98±0.56
9l	NCH_3	O	OCH_3	H	80.27±3.82	5.97±0.73	1.38±0.47
9m	NCH_3	O	OH	H	73.65±5.25	6.90±0.45	3.53±0.23
9n	S	NCH_3	H	H	45.59±4.48	n.t.[c]	1.64±0.17
9o	O	NCH_3	H	H	65.73±4.34	8.56±0.82	2.79±0.09
HL_5	-	-	-	-	64.75±4.86	9.78±1.23	0.64±0.43
HL_{12}	-	-	-	-	67.78±3.48	8.75±1.09	1.10±0.06
Curcumin	-	-	-	-	56.81±0.46	8.48±1.14	1.56±0.26
Trolox	-	-	-	-	n.t.[c]	n.t.[c]	1.00±0.24

[a] The thioflavin-T fluorescence method was used. The values are expressed as the mean of three independent measurements. All values were obtained at a compound concentration of 20 μM.
[b] The mean of the three independent experiments.
[c] n.t. means not tested.

3.2.2. Trolox-equivalent antioxidant capacity assay

The antioxidant activities of compounds **9a**-**9o** were evaluated with Trolox-equivalent antioxidant capacity (TEAC) assay, which is based on the generation and detection of a blue -colored cation ($ABTS^{\bullet+}$, 2, 2'-azino-bis(3-ethyl-benzothiazoline-6-sulfonic acid) radical cation) using Trolox as a a control[37,38]. The TEAC values were expressed as Trolox equivalents calculated from the ratio of the slopes of the concentration-response curves, the antioxidant vs Trolox (TEAC value = 1.00).

As shown in Table 1, all the compounds displayed excellent $ABTS^{\bullet+}$ scavenging activities with TEAC values ranging from 1.31 to 6.03, and the majority of them were superior to that of curcumin, **HL_5** and **HL_{12}** (TEAC values of 0.64, 1.10, 1.56 respectively). In particular, four 3-hydroxy-4-pyranone derivatives **9a**, **9c**, **9i**, **9k** displayed very potent radical scavenging activities with TEAC values of 4.03, 4.29, 6.03 and 4.98 respectively. The primary SAR indicated that modification of benzothiazole ring significantly affected the activity with benzoxazole and N-Me-benzoimidazole, when the compounds containing benzoxazole moieties exerted similar antioxidant activity, while N-Me benzoimidazole derivatives displayed compromised activity (**9a**, **9c** vs **9e**). As expected, in comparison with unsubstituted compounds (**9a**, **9e**), the

RSC Advances Accepted Manuscript

introduction of hydroxy moiety into R_2 position of benzothiazole ring resulted in a remarkable enhancement in activity (**9i**, **9m**), while the bromo and methoxy moities were not favorable for activity (**9h**, **9j**). The methyl moiety in R_1 pyranone ring also decreased the antioxidant capacities obviously (**9a** vs **9b**, **9c** vs **9d**), indicating the detrimental steric effect on antioxidant activity.

3.2.3. Metal chelating property

The metal chelating activities of compounds **9a-o** were measured by UV-Vis spectroscopy using deferiprone and maltol as positive control. As expected, all the compounds displayed good metal chelating activities similar to deferiprone and maltol. As shown in Figure S1 (Supporting Information), significant red shift was observed in UV-Vis spectra when Cu^{2+}, Zn^{2+}, Fe^{2+}, Fe^{3+} was mixed with the compounds **9a-o**, deferiprone and maltol, indicating the formation of metal ion complex. These results confirmed that the 3-hydroxy-4-pyridinone or 3-hydroxy-4-pyranone moiety was essential for metal chelating activity.

3.2.4. The choice of drug candidates

Based on the above biological evaluation results, compounds **9c** and **9i** exhibited the most desirable triple functions (IC_{50} values of 7.05, 5.06 μM for Aβ self-aggregation inhibition, TEAC values of 4.29, 6.03 for $ABTS^{\bullet+}$ scavenging activity and potent chelating activities with copper, iron and zinc ions). Therefore, the two compounds were chosen as drug candidates for further biological evaluation.

3.2.5. Inhibition of self-induced Aβ aggregation monitored by TEM

To further confirm the ability of compounds **9c** and **9i** against $A\beta_{1-42}$ aggregation, the inhibitory activities of them were monitored by transmission electron microscopy (TEM) using curcumin as a positive control. After incubated for 24h at 37°C, compared to $A\beta_{1-42}$ without incubation (Figure 4a), $A\beta_{1-42}$ alone aggregated into well-defined Aβ fibrils (Figure 4b). On the contrary, few Aβ fibrils were observed in the presence of compounds **9c** and **9i** (Figure 4d and Figure 4e) under identical conditions, which were similar to that of curcumin (Figure 4c). Therefore, the results of TEM and ThT assay proved that compounds **9c** and **9i** could effectively inhibit self-induced $A\beta_{1-42}$ fibril formation.

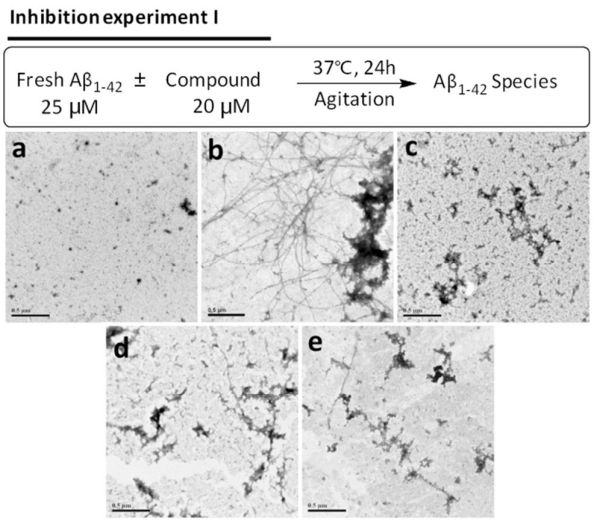

Figure 4. (TOP) Scheme of inhibition experiments on self-induced Aβ aggregation. TEM images. (a) $A\beta_{1-42}$, 0 h. (b) $A\beta_{1-42}$ alone. (c) $A\beta_{1-42}$+curcumin. (d) $A\beta_{1-42}$+**9c**. (e) $A\beta_{1-42}$+**9i**.

3.2.6. Disaggregation of self-induced Aβ aggregation

The ability of compounds **9c** and **9i** to disaggregate self-induced $A\beta_{1-42}$ aggregation fibrils was investigated by thioflavin T (ThT) fluorescence assay and transmission electron microscopy (TEM) using curcumin as positive control. $A\beta_{1-42}$ fibrils were generated by incubating fresh $A\beta_{1-42}$ for 24 h at 37 °C (Figure 5b), then curcumin, compounds **9c** or **9i** was added to the sample and incubated for another 24 h at 37°C with constant agitation.

The ThT binding assay revealed that both compound **9c** and **9i** could effectively disaggregate previously formed self-induced $A\beta_{1-42}$ fibrils (49.3% and 47.9%, respectively), which were a slightly better than curcumin (53.6%) (Figure S2).

The TEM assay results in Figure 5c, 5d, 5e also showed that compounds **9c** and **9i** were capable of disassembling the $A\beta_{1-42}$ fibrils from self-mediated aggregation with similar acitivity to that of curcumin.

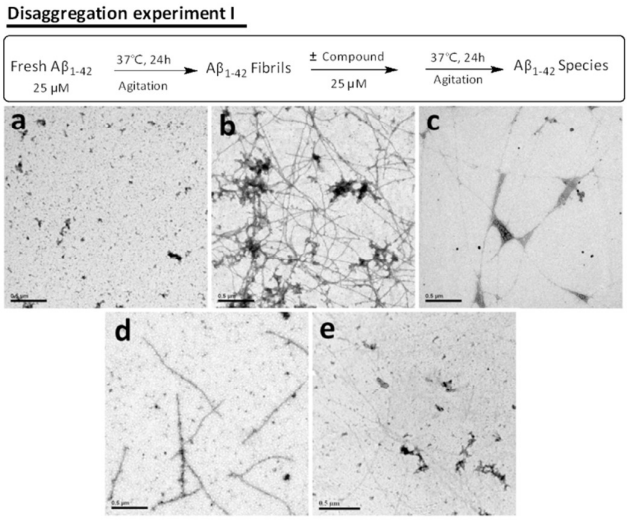

Figure 5. (Top) Scheme of disaggregation experiments on self-induced $A\beta_{1-42}$ aggregation. TEM images. (a) $A\beta_{1-42}$, 0 h. (b) $A\beta_{1-42}$ alone. (c) $A\beta_{1-42}$+ curcumin. (d) $A\beta_{1-42}$+**9c**. (e) $A\beta_{1-42}$+**9i**.

3.2.7. Metal-chelating Characteristics of 9c, 9i

The ability of **9c** and **9i** to chelate biometals was studied by UV-vis spectroscopy (Figure 6). After $ZnCl_2$, $FeSO_4$, $CuCl_2$ or $FeCl_3$ was added to a solution of **9c**, an obvious drop of absorbance at 341 nm was observed (Figure 6a) indicating the formation of **9c**-Zn^{2+}, **9c**-Fe^{2+}, **9c**-Cu^{2+}, **9c**-Fe^{3+} complex. Similarly, Figure 5b revealed that compound **9i** was potent chelator for biometals Cu^{2+}, Fe^{3+}, Zn^{2+} and Fe^{2+}.

The stoichiometry of the **9c** and **9i** with copper complex was determined using Job's method. A series of solutions were prepared, in which the total concentration of compound **9c** or **9i** and $CuCl_2$ remained constant while their proportions varied. The UV spectroscopys of **9c** with $CuCl_2$ complex at different concentrations were evaluated and the absorbance changes at 341 nm were plotted. As illustrated in Figure 6c, the two straight lines intersected at a mole fraction of 0.686, which implied a 2:1 **9c**-Cu (II) complex. Similarly, the UV spectroscopy of **9i** with $CuCl_2$ complex was shown in Figure 6d with the absorbance changes at 370 nm being plotted.

RSC Advances Accepted Manuscript

This journal is © The Royal Society of Chemistry 20xx

The Job plot revealed a break at 0.651, indicating a 2:1 stoichiometry for the **9i**–Cu (II) complex.

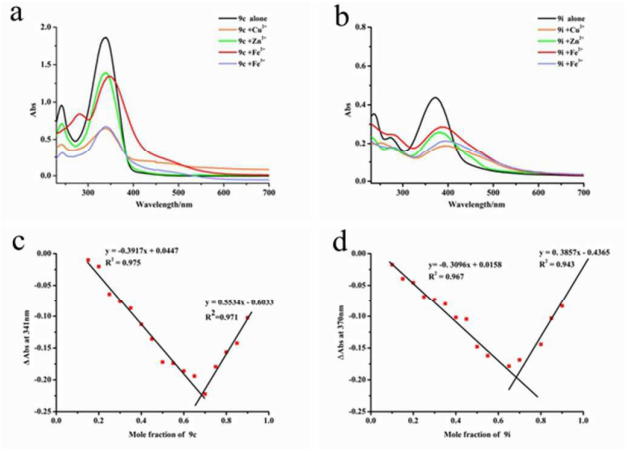

Figure 6. (a) UV-vis spectra of compounds **9c** with biometals. (b) UV-vis spectra of compounds **9i** with biometals. [**9c**], [**9i**]=50μM, [Cu^{2+}], [Zn^{2+}], [Fe^{2+}], [Fe^{3+}] = 25 μM. (c) Determination of the stoichiometry of complex **9c**–Cu (II) by Job's method. (d) Determination of the stoichiometry of complex **9i**–Cu (II) by Job's method.

3.2.8. Inhibition of Cu^{2+}-induced Aβ aggregation

To investigate the ability of 2-subsituted benzothiazole derivatives to inhibit Cu (II)-induced $Aβ_{1-42}$ aggregation, the ThT fluorescence and TEM experiments were carried out. The ThT fluorescence assay revealed that the Cu^{2+} led to a reduced ThT fluorescence in comparison with Aβ self (83.7%, Figure S3), probably due to the emission quenched by the paramagnetic Cu^{2+} ions-induced formation of nonfibrillar Aβ aggregates.[41,42] The addition of **9c** and **9i** resulted in a dramatic decrease of ThT fluorescence (27.0% and 24.1% respectively), indicating their excellent activities to inhibit Cu^{2+} induced $Aβ_{1-42}$ aggregation in comparison with CQ (46.3%).

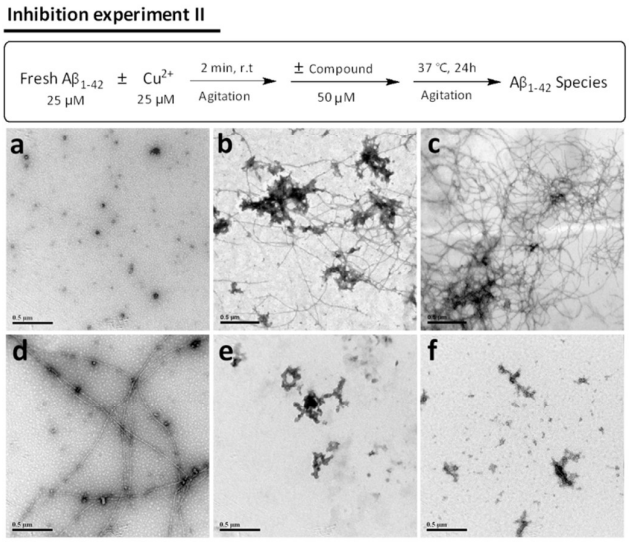

Figure 7. (Top) Scheme of inhibition experiment on copper induced $Aβ_{1-42}$ aggregation. TEM images. (a) $Aβ_{1-42}$, 0 h. (b) $Aβ_{1-42}$ alone, 24h. (c) $Aβ_{1-42}$ + Cu, 24h. (d) $Aβ_{1-42}$+Cu + CQ. (e) $Aβ_{1-42}$+Cu +**9c**. (f). $Aβ_{1-42}$+Cu +**9i**.

The TEM showed that a significant amount of fibrillogenesis (Figure 7c) was observed in the presence of Cu (II) than for $Aβ_{1-42}$ alone (Figure 7b), and fewer Aβ fibrils were observed when **9c** (Figure 7e) or **9i** (Figure 7f) was added to the samples, which were similar to that of CQ added the sample (Figure 7d). The above observation suggested that compounds **9c** and **9i** were potent copper chelators with ability to inhibit copper-induced Aβ aggregations.

3.2.9. Disaggregation of Cu- Induced $Aβ_{1-42}$ Aggregation

The capability of compounds **9c** and **9i** to disaggregate copper-induced Aβ aggregation fibrils was investigated by Th-T fluorescence assay and TEM as well. $Aβ_{1-42}$ fibrils were generated by incubating fresh $Aβ_{1-42}$ with 1.0 equiv of Cu^{2+} for 24 h at 37 °C with constant agitation (Figure 8b). Compound **9c**, **9i** or clioquinol was then added to the sample and incubated for another 24 h at 37°C.

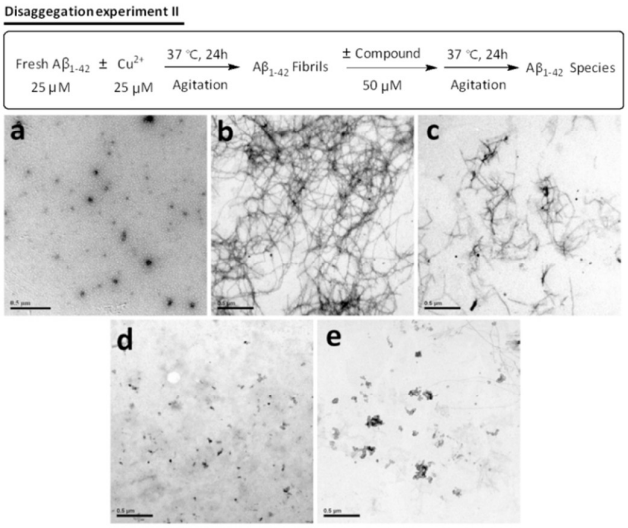

Figure 8. (Top) Scheme of disaggregation experiments on copper-induced $Aβ_{1-42}$ aggregation. TEM images. (a) $Aβ_{1-42}$, 0 h.(b) $Aβ_{1-42}$ +Cu. (c) $Aβ_{1-42}$+Cu + CQ. (d) $Aβ_{1-42}$+Cu +**9c**. (e) $Aβ_{1-42}$+Cu +**9i**.

As shown in Figure S3, the ThT binding assay demonstrated that both compound **9c** and **9i** was able to resolve Aβ fibrils (30.9% and 26.8% disaggregation respectively).

In comparison with the well-defined Aβ fibrils in Figure 8b, noticeably fewer $Aβ_{1-42}$ fibrils were observed when CQ or **9c** or **9i** was added to the samples (Figure 8c, 8d and 8e), indicating **9c** and **9i** could efficiently disassemble copper-induced $Aβ_{1-42}$ fibrils.

3.2.10. Cytotoxicity

To investigate the safety profile of these benzothiazole derivatives, the cytotoxicity of compounds **9c** and **9i** against human glioma U251 cells was evaluated by SRB (sulforhodamine B) assay, and HL_5 and HL_{12} was used reference compounds. As illustrated in Figure 9, compounds **9c** and **9i** did not show obvious cytotoxicity at concentrations 50 μM after 24h incubation, while for the controls HL_5 and HL_{12}, they demonstrated obvious toxicity to U251 cells at concentrations 10 μM. These results indicated that compounds **9c** and **9i** possesssed more favorable safety profile than HL_5 and HL_{12} and were suitable for further development for the treatment of AD.

RSC Advances Accepted Manuscript

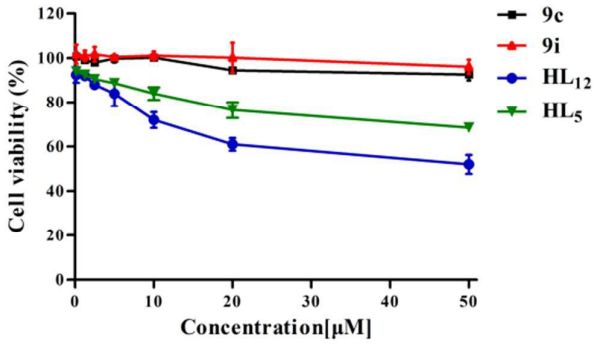

Figure 9 Effects of **9c, 9i**, $\mathbf{HL_5}$ and $\mathbf{HL_{12}}$ on U251 cell viability. Data represent mean ±SD.

4 CONCLUSIONS

A novel series of 2-substituted-benzothiazole were designed as potential MTDLs for AD therapy through combination of metal chelating moiety 3-hydroxy-4-pyranone (or 3-hydroxy-4-pyridinone) and benzothiazole moiety from ThT with vinyl linker. Most of these compounds exhibited more potent $A\beta_{1\text{-}42}$ aggregation inhibitory activity and more efficient $ABTS^{\bullet+}$ scavenging capability than that of curcumin and two positive controls $\mathbf{HL_5}$ and $\mathbf{HL_{12}}$, which confirmed the rationality of our drug design strategy. The further in vitro biological evaluation of two promising compounds **9c** and **9i** revealed that they were novel MTDLs with triple functions. Moreover, the cytotoxic evalution also demonstrated that **9c** and **9i** were not toxic to human glioma U251 cells up to 50 μM, which were much better than $\mathbf{HL_5}$ and $\mathbf{HL_{12}}$. All the above results indicated that these new hybrids were interesting MTDLs with potential to be developed as therapeutic agents against AD.

5. Experimental section

General Methods and Materials

All reagents and solvents used were reagent grade and purchased from commercial resources. $A\beta_{1\text{–}42}$ was purchased from Chinese Peptide Company. Melting points were determined with a B-540 Buchi melting-point apparatus. ^{1}H NMR and ^{13}C NMR were recorded on a Brüker Advance DMX 500 MHz or DMX 400 MHz spectrometer. Coupling constants (*J*) were expressed in hertz (Hz) and chemical shifts (δ) of NMR were reported in parts per million (ppm) units relative to an internal control (TMS). Low resolution mass spectras (ESI-MS) were gathered on a Finnigan LCQ DecaXP ion trap mass spectrometer. UV–visible spectras were recorded on a U-3010 spectrophotometer. TECAN F200 reader was used for radical scavenging assay, ThT fluorescence assay. JEM1200EX transmission electron microscope was used for $A\beta_{1\text{–}42}$ aggregation and disaggreagation assay. All targeted compounds were purified to ⩾94% purity as determined by Agilent 1260 series HPLC systems with a Eclipse XDB-C18 (4.6 ×250 mm, 5 μm); 20.0 μL injection volume; flow rate of 1.0 mL/min; (Mobile phase: A: H_2O, B: MeCN) with a UV detector set at 254 nm.

General procedure for the synthesis of compounds 11a and 11b

To a mixture of compound **10a** (42.2 mmol) and K_2CO_3 (12.2 g, 88.7 mmol) in dry DMF (15 mL) was added PMB-Cl (7.1 mL, 52.8 mmol) in drop wise. The mixture was stirred for 2 h at 80 ℃ and quenched with 10 mL H_2O. After extraction with EtOAc (3×20mL), the combined organic layer was washed with water, saturared saline and dried over Na_2SO_4. The solvent was removed in vacuo and the residue was recrystallizated with ethyl acetate to afford compound **11a.** 2-(hydroxymethyl)-5- ((4-methoxybenzyl)oxy)-4H-pyran-4-one (**11a**). White solid, yield 84.1%. ^{1}H NMR (500 MHz, DMSO) /δ (ppm)**:** 8.14 (s, 1H, *H*-6), 7.34 (d, 2H , *J* = 8.0 Hz, Ph-*H*-2', *H*-6'), 6.95 (d, 2H, *J* = 7.5 Hz, Ph-*H*-3', *H*-5'), 6.30 (s, 1H, *H*-3), 5.67 (t, 1H, *J* = 5.5 Hz, O*H*), 4.85 (s, 2H, Ph-CH_2) , 4.29 (d, 2H, *J* = 5.5 Hz, CH_2OH) , 3.75 (s, 3H, OCH_3) , ESI-MS (m/z) : 263.2 $[M + H]^+$.

6-(hydroxymethyl)-3-((4-methoxybenzyl)oxy)-2-methyl-4H-pyran-4-one (**11b**). White solid, yield 64.0% . ^{1}H NMR (400 MHz , $CDCl_3$) /δ (ppm) : 7.31 (d , 2H , *J* = 8.4 Hz , Ph-*H*-2', *H*-6') , 6.87 (d, 2H, *J* = 8.8 Hz, Ph-*H*-3', *H*-5') , 6.45 (s, 1H, *H*-5) , 5.07 (s, 2H, Ph-CH_2) , 4.44 (s, 2H, CH_2OH) , 3.80 (s, 3H, OCH_3) , 2.05 (s, 3H, CH_3). ESI-MS (m/z) : 277.3 $[M + H]^+$.

General procedure for the synthesis of compounds 12a and 12b

A mixture of **11a** (2.62 g, 10.0 mmol) and manganese (IV) oxide (13.04g, 150.0 mmol) suspended in $CHCl_3$ (65 mL) was reflux overnight. After cooling to r.t., the reaction mixture was filtered through Celite and the filtrate was concentrated to dryness. The residue was purified by silica gel chromatography eluting with PE/EtOAc to afford **12a** as a white solid. Yield 45.2%. 5-((4-methoxybenzyl)oxy)-4-oxo-4H-pyran-2-carbaldehyde (**12a**). ^{1}H NMR (400 MHz, $CDCl_3$) /δ(ppm): 9.64 (s, 1H, C*H*O), 7.65 (s, 1H, *H*-6), 7.32 (d, 2H, *J* = 8.8 Hz, Ph-*H*-2, *H*-6'), 6.98 (s, 1H, *H*-3), 6.91 (d, 2H, *J* = 8.8 Hz, Ph-*H*-3', *H*-5'), 5.07 (s, 2H, Ph-CH_2), 3.81 (s, 3H, OCH_3). ESI-MS (m/z): 261.1 $[M + H]^+$.

5-((4-methoxybenzyl)oxy)-6-methyl-4-oxo-4H-pyran-2-carbaldehyde (**12b**). Yellow solid, yield 66.3%. ^{1}H NMR (500 MHz, $CDCl_3$) /δ (ppm): 9.55 (s, 1H, C*H*O), 7.25 (d, 2H, *J* = 8.5 Hz, *H*-2', *H*-6'), 6.89 (s, 1H, H-5), 6.89 (d, 2H, *J* = 8.5 Hz, *H*-3', *H*-5'), 5.09 (s, 2H, Ph-CH_2), 3.74 (s, 3H, OCH_3), 2.12 (s, 3H, CH_3). ESI-MS (m/z): 275.3 $[M + H]^+$.

General procedure for the synthesis of compounds 13a-g, 13j, 13l

Compound **12a** (440.0 mg, 1.69 mmol) and 2-methylbenzothiazole (252.0mg, 1.69 mmol) were mixed with acetic anhydride (3.52 mL) and acetic acid (1.76 mL). The mixture was stirred for 20 min at 145 ℃ under microwave condition. After removal of solvent, the residue was partitioned with EtOAc (20 mL) and water (20 mL). The aquoeus solution was extracted with EtOAc (20 mL×3) and the combined organic phase was washed with brine, and dried over Na_2SO_4. After concentration to dryness, the residue was purified by silica gel chromatography eluting with PE/EtOAc to afford **13a** as a yellow solid. Yield 52.4%. (E)-6-(2-(benzo[d]thiazol-2-yl)vinyl)-4-oxo-4H-pyran-3-yl acetate (**13a**). ^{1}H NMR (400 MHz, $CDCl_3$)/ δ (ppm): 8.08 (d, 1H, *J* = 8.0 Hz, *H*-4'), 7.94 (s, 1H, *H*-6), 7.92 (d, 1H, *J* = 7.6 Hz, *H*-7'), 7.63 (d, 1H, *J* = 16.0 Hz, CH=CH_a), 7.56-7.52 (m, 1H, *H*-5'), 7.47-7.43 (m, 1H, *H*-6'), 7.19 (d, 1H, *J* = 16.0 Hz, CH_b=CH), 6.56 (s, 1H, *H*-3), 2.35 (s, 3H, COCH_3). ESI-MS (m/z): 314.3 $[M + H]^+$.

(E)-6-(2-(benzo[d]thiazol-2-yl)vinyl)-2-methyl-4-oxo-4H-pyran-3-yl acetate (**13b**) Yellow solid, yield 63.7%. ^{1}H NMR (400 MHz, $CDCl_3$) /

This journal is © The Royal Society of Chemistry 20xx

RSC Advances Accepted Manuscript

δ (ppm): 8.07 (d, 1H, *J* = 8.0 Hz, *H*-4'), 7.86 (d, 1H, *J* = 7.6 Hz, *H*-7'), 7.64 (d, 1H, *J* = 16.0 Hz, CH=C*H*$_a$), 7.55-7.52 (m, 1H, *H*-5'), 7.47-7.42 (m, 1H, *H*-6'), 7.14 (d, 1H, *J* = 16.0 Hz, C*H*$_b$=CH), 6.48 (s, 1H, *H*-3), 2.36 (s, 3H, C*H*$_3$), 2.35 (s, 3H, COC*H*$_3$). ESI-MS (m/z): 328.2 $[M+H]^+$.

(E)-6-(2-(benzo[d]oxazol-2-yl)vinyl)-4-oxo-4H-pyran-3-yl acetate (**13c**). Yellow solid, yield 54.1%. ^{1}H NMR (500 MHz, DMSO-d6)/δ (ppm): 8.56 (s, 1H, *H*-6), 7.83 (d, 1H, *J* = 7.5 Hz, *H*-4'), 7.78 (d, 1H, *J* = 8.0 Hz, *H*-7'), 7.66 (d, 1H, *J* = 16.0 Hz, CH=C*H*$_a$), 7.51-7.49 (m, 1H, *H*-5'), 7.46-7.43 (m, 1H, *H*-6'), 7.39 (d, 1H, *J* = 16.0 Hz, C*H*$_b$=CH), 6.98 (s, 1H, *H*-3), 2.28 (s, 3H, COC*H*$_3$). ESI-MS (m/z): 298.2 $[M + H]^+$.

(E)-6-(2-(benzo[d]oxazol-2-yl)vinyl)-2-methyl-4-oxo-4H-pyran-3-yl acetate (**13d**). Yellow solid, yield 52.2%. ^{1}H NMR (400 MHz, $CDCl_3$)/δ (ppm): 7.78 (d, 1H, *J* = 8.8 Hz, *H*-4'), 7.57 (d, 1H, *J* = 8.4 Hz, *H*-7'), 7.44-7.37 (m, 2H, *H*-5', *H*-6'), 7.32 (s, 2H, C*H*=C*H*), 6.50 (s, 1H, *H*-3), 2.37 (s, 3H, C*H*$_3$), 2.36 (s, 3H, COC*H*$_3$). ESI-MS (m/z): 312.2 $[M + H]^+$.

(E)-6-(2-(1-methyl-1H-benzo[d]imidazol-2-yl)vinyl)-4-oxo-4H-pyran-3-yl acetate (**13e**). Yellow solid, yield 46.6%. ^{1}H NMR (400 MHz, $CDCl_3$) /δ (ppm): 7.94 (s, 1H, *H*-6), 7.80-7.78 (m, 1H, *H*-4'), 7.63 (d, 1H, *J* = 16.0 Hz, CH=C*H*$_a$), 7.41-7.31 (m, 4H, C*H*$_b$=CH, *H*-7', *H*-5', *H*-6'), 6.55 (s, 1H, *H*-3), 3.92 (s, 1H, NC*H*$_3$), 2.35 (s, 3H, COC*H*$_3$). ESI-MS (m/z): 311.3 $[M + H]^+$.

(E)-2-methyl-6-(2-(1-methyl-1H-benzo[d]imidazol-2-yl)vinyl)-4-oxo-4H-pyran-3-yl acetate (**13f**). Yellow solid, yield 32.6%. ^{1}H NMR (400 MHz, $CDCl_3$)/δ (ppm): 7.79-7.77 (m, 1H, *J* = 7.2 Hz, *H*-7'), 7.55 (d, 1H, *J* = 16.0 Hz, CH=C*H*$_a$), 7.41-7.33 (m, 4H, C*H*$_b$=CH, *H*-7', *H*-5', *H*-6'), 6.49 (s, 1H, *H*-3), 3.92 (s, 1H, NC*H*$_3$), 2.37 (s, 3H, C*H*$_3$), 2.36 (s, 3H, COC*H*$_3$). ESI-MS (m/z): 325.2 $[M + H]^+$.

(E)-6-(2-(6-methoxybenzo[d]thiazol-2-yl)vinyl)-4-oxo-4H-pyran-3-yl acetate (**13g**) Yellow solid, yield 35.3%. ^{1}H NMR (400 MHz, $CDCl_3$)/δ (ppm): 7.95 (d, 1H, *J* = 8.8 Hz, *H*-4'), 7.93 (s, 1H, *H*-6), 7.60 (d, 1H, *J* = 16.0 Hz, CH=C*H*$_a$), 7.34 (d, 1H, *J* = 2.4 Hz, *H*-7'), 7.14 (dd, 1H, J_1 = 9.2 Hz, J_2 = 2.8 Hz, *H*-5'), 7.08 (d, 1H, *J* = 16.0 Hz, C*H*$_b$=CH), 6.53 (s, 1H, *H*-3), 3.91 (s, 3H, OC*H*$_3$), 2.35 (s, 3H, COC*H*$_3$). ESI-MS (m/z): 344.3 $[M +H]^+$.

(E)-6-(2-(6-bromobenzo[d]thiazol-2-yl)vinyl)-4-oxo-4H-pyran-3-yl acetate (**13h**) Yellow solid**,** yield 45.6%. ^{1}H NMR (500 MHz, $CDCl_3$) /δ (ppm): 8.05 (d, 1H, *J* = 1.5 Hz , *H*-7'), 7.94 (s, 1H, *H*-6), 7.91 (d, 1H, *J* = 8.5 Hz, *H*-4'), 7.64 (dd, 1H, J_1 = 9.0 Hz, J_2 = 2.0 Hz, *H*-5'), 7.59 (d, 1H, *J* = 16.0 Hz, CH=C*H*$_a$), 7.18 (d, 1H, *J* = 16.0 Hz, C*H*$_b$=CH), 6.58 (s, 1H, *H*-3), 2.35 (s, 3H, COC*H*$_3$). ESI-MS (m/z): 393.2 $[M + H]^+$.

(E)-6-(2-(6-methoxybenzo[d]oxazol-2-yl)vinyl)-4-oxo-4H-pyran-3-yl acetate (**13j**) Yellow solid**,** yield 35.6%. ^{1}H NMR (500 MHz, $CDCl_3$) /δ (ppm): 7.95 (s 1H, *H*-6), 7.76 (d, 1H, *J* = 9.0, *H*-4'), 7.29 (d, 1H, *J* = 16.0 Hz, CH=C*H*$_a$), 7.23 (d, 1H, *J* = 15.5 Hz, C*H*$_b$=CH), 6.77 (dd, 1H, J_1 = 9.0 Hz, J_2 =2.5 Hz ,*H*-5'), 6.66(sd,1H,*J* = 3.0,H-7'), 6.55(s, 1H, *H*-3), 3.75 (s, 3H, OC*H*$_3$), 2.36 (s, 3H, COC*H*$_3$). ESI-MS (m/z): 328.4 $[M + H]^+$.

(E)-6-(2-(6-methoxy-1-methyl-1H-benzo[d]imidazol-2-yl)vinyl)-4-oxo-4H-pyran-3-yl acetate (**13l**) Yellow solid**,** yield 42.8%. ^{1}H NMR (500 MHz, $CDCl_3$) /δ (ppm): 7.93 (s 1H, *H*-6), 7.70 (d, 1H, *J* = 9.0, *H*-4'), 7.65 (d, 1H, *J* = 15.5 Hz, CH=C*H*$_a$), 7.36 (d, 1H, *J* = 15.5 Hz, C*H*$_b$=CH), 7.01 (dd, 1H, J_1 = 8.0 Hz, J_2 =2.0 Hz ,*H*-5'), 6.80 (d, 1H, *J* = 2.5 Hz, *H*-7'), 6.51(s, 1H, *H*-3), 3.91 (s, 3H, OC*H*$_3$), 3.90 (s, 3H, NC*H*$_3$), 2.35 (s, 3H, COC*H*$_3$).

General Procedure for the Preparation of 9a-9h, **9j**, **9l**

A mixture of **13a** (0.46 mmol) and anhydrous K_2CO_3 (222mg, 1.60 mmol) in 15 mL MeOH was stirred for 0.5 h at room temperature. The solvent was removed under reduced pressure and the residue was acidified with diluted HCl. The solution was extracted with ethyl acetate (20 mL×3) and the combined organic phase was washed with brine, dried over Na_2SO_4. After concentration to dryness, the residue was purified by silica gel chromatography to furnish solid products **9a-9h**, **9j**, **9l**

(E)-2-(2-(benzo[d]thiazol-2-yl)vinyl)-5-hydroxy-4H-pyran-4-one **(9a).** Yellow solid, yield 80.1%. ^{1}H NMR (500 MHz, DMSO-d_6)/δ (ppm): 9.35（s, 1H, O*H*）, 8.16 (d, 1H, *J* = 8.0 Hz, *H*-4'), 8.12 (s, 1H, *H*-6), 8.05 (d, 1H, *J* = 8.0 Hz, *H*-7'), 7.62-7.47 (m, 4H, *H*-5', *H*-6', C*H*=C*H*), 6.81 (s, 1H, *H*-3). ^{13}C NMR (125 MHz, DMSO-d_6)/δ (ppm): 175.1, 165.3, 160.1, 154.6, 147.6, 140.6, 136.0, 129.1, 128.2, 128.1, 127.4, 123.7, 115.9. ESI-MS (m/z): 272.5 $[M + H]^+$. HPLC purity = 98.42%, Rt 14.84min.

(E)-6-(2-(benzo[d]thiazol-2-yl)vinyl)-3-hydroxy-2-methyl-4H-pyran-4-one(**9b**) Yellow solid, yield 70.1% . ^{1}H NMR (400 MHz , $CDCl_3$)/δ (ppm): 8.08 (d, 1H, *J* = 7.6 Hz, H-4'), 7.92 (d, 1H, *J* = 8.0 Hz, *H*-7'), 7.66 (d, 1H, *J* = 15.2 Hz, CH=C*H*$_a$) , 7.55 (t, 1H, *J* = 7.2 Hz, *H*-5'), 7.47 (t, 1H, *J* = 7.2 Hz, H-6'), 7.18 (d, 1H, *J* = 15.6 Hz, C*H*$_b$=CH), 6.52 (s, 1H, H-3), 2.47 (s, 3H, C*H*$_3$). ^{13}C NMR (100 MHz, $CDCl_3$)/δ (ppm): 170.2, 163.9, 153.5, 152.9, 147.8, 147.1, 140.1, 134.9, 127.8, 126.9, 126.4, 123.6, 121.8, 114.6, 18.3. ESI-MS (m/z): 286.5 $[M + H]^+$. HPLC purity = 98.83%, Rt 20.81 min.

(E)-2-(2-(benzo[d]oxazol-2-yl)vinyl)-5-hydroxy-4H-pyran-4-one (**9c**) Yellow solid, yield 78.4%. ^{1}H NMR (400 MHz, $CD_3OD/CDCl_3$) /δ (ppm): 7.88 (s, 1H, *H*-6), 7.70 (d, 1H, *J* =7.2 Hz, *H*-4'), 7.52 (d, 1H, *J* = 7.2 Hz , *H*-7'), 7.30-7.24 (m, 4H, *H*-5', *H*-6', C*H*=C*H*), 6.53 (s, 1H, *H*-3). ^{13}C NMR (100 MHz, $CD_3OD/CDCl_3$)/δ (ppm) : 168.7, 164.5, 163.5, 159.6, 154.3, 145.5, 143.0, 133.2, 130.5, 129.1, 124.5, 124.2, 118.1, 114.6. ESI-M(m/z): 256.5 $[M + H]^+$. HPLC purity = 98.26%, Rt 15.07 min.

(E)-6-(2-(benzo[d]oxazol-2-yl)vinyl)-3-hydroxy-2-methyl-4H-pyran-4-one (**9d**). Yellow solid, yield 77.4%. ^{1}H NMR (400 MHz, $CD_3OD/CDCl_3$)/δ (ppm): 7.71 (d, 1H, *J* = 7.2 Hz, *H*-4'), 7.53 (d, 1H, *J* = 7.2 Hz, *H*-7'), 7.39-7.30 (m, 4H, *H*-5', *H*-6', C*H*=C*H*), 6.50 (s, 1H, *H*-3), 2.42 (s, 3H, C*H*$_3$). ^{13}C NMR (100 MHz, $CD_3OD/CDCl_3$)/δ (ppm): 173.3, 169.1, 167.6, 156.7, 153.4, 146.8, 135.3, 130.5, 129.1, 124.2, 123.9 , 120.3 , 117.4 , 114.6 , 15.21. ESI-MS (m/z): 270.4 $[M + H]^+$. HPLC purity = 98.93%, Rt 18.44 min.

(E)-5-hydroxy-2-(2-(1-methyl-1H-benzo[d]imidazol-2-yl)vinyl)-4H-pyran-4-one (**9e**). Yellow solid, yield 90.0%. ^{1}H NMR (400 MHz, $CD_3OD/CDCl_3$)/δ (ppm): 8.0 (brs, 1H, OH), 7.85 (s, 1H, *H*-6), 7.65 (d, 1H, *J* = 8.8 Hz, *H*-4'), 7.39-7.36 (m, 2H, CH=C*H*$_a$, *H*-7'), 7.30-7.24 (m, 3H, *H*-5', *H*-6', C*H*$_b$=CH), 6.57 (s, 1H, *H*-3), 3.84 (s, 3H, NC*H*$_3$). ^{13}C NMR (100 MHz, $CD_3OD/CDCl_3$)/δ (ppm): 170.9, 165.8, 159.0, 157.3, 152.5, 146.3, 144.1, 139.8, 130.9, 127.9, 127.5, 123.5, 123.1, 113.7, 33.7. ESI-MS(m/z): 269.5 $[M + H]^+$. HPLC purity = 98.30%, Rt 13.30min.

(E)-3-hydroxy-2-methyl-6-(2-(1-methyl-1H-benzo[d]imidazol-2-yl) vinyl)-4H-pyran-4-one (**9f**). Yellow solid, yield 65.6%. ^{1}H NMR (400 MHz , DMSO-d_6)/δ (ppm): 7.65 (d, 1H, *J* = 7.6 Hz, *H*-7'), 7.61 (d, 1H, *J* =7.6 Hz, *H*-4'), 7.55 (s, 2H, C*H*=C*H*), 7.31-7.23 (m, 2H, *H*-5', *H*-6'), 6.75 (s, 1H, *H*-3), 3.96 (s, 3H, NC*H*$_3$), 2.38 (s, 3H, C*H*$_3$). ^{13}C NMR (100

RSC Advances Accepted Manuscript

MHz, DMSO-d_6)/δ (ppm): 175.8, 159.1, 149.5, 148.9, 146.2, 143.2, 136.7, 126.9, 123.3, 123.0, 120.3, 119.4, 113.4, 111.0, 30.2, 14.6. ESI-MS (m/z): 283.4 $[M + H]^+$. HPLC purity = 96.18%, Rt 15.23min.

(E)-5-hydroxy-2-(2-(6-methoxybenzo[d]thiazol-2-yl)vinyl)-4H-pyran-4-one (**9g**). Yellow solid, yield 90.9%. ^{1}H NMR (400 MHz, DMSO-d_6)/δ (ppm): 9.31 (s, 1H, O*H*), 8.10 (s, 1H, *H*-6), 7.93 (d, 1H, *J* = 9.2 Hz, *H*-4′), 7.73 (d, 1H, *J* = 2.0 Hz, *H*-7′), 7.57 (d, 1H, *J* = 16.0 Hz, CH=C*H*$_a$), 7.40 (d, 1H, *J* = 16.0 Hz, C*H*$_b$=CH), 7.17 (dd, 1H, J_1 = 8.8 Hz, J_2 = 2.4 Hz, *H*-5′), 6.78 (s, 1H, *H*-3), 3.86 (s, 3H, OC*H*$_3$). ^{13}C NMR (100 MHz, DMSO-d_6)/δ (ppm): 174.3, 161.9, 159.6, 158.6, 148.3, 146.7, 139.9, 136.9, 127.5, 127.2, 124.2, 117.0, 114.7, 105.2, 56.2. ESI-MS (m/z): 302.4 $[M +H]^+$. HPLC purity = 98.92%, Rt 15.79min.

(E)-2-(2-(6-bromobenzo[d]thiazol-2-yl)vinyl)-5-hydroxy-4H-pyran-4-one (**9h**). Yellow solid, yield 76.2%. ^{1}H NMR(400 MHz, DMSO-d_6)/δ (ppm)：9.49 (brs, 1H, O*H*), 8.49 (d, 1H, *J* = 2.0 Hz, *H*-6), 8.16 (s, 1H, *J* = 1.6 Hz, *H*-7′), 7.99 (d, 1H, *J* = 8.8 Hz, *H*-4′), 7.72 (dd, 1H, J_1= 8.4 Hz, J_2 = 2.0 Hz, *H*-5′), 7.64 (d, 2H, *J* = 16.4 Hz, CH=C*H*$_a$), 7.55 (d, 2H, *J* = 16.4 Hz, C*H*$_b$=CH), 6.83 (s, 1H, *H*-3). ^{13}C NMR (100 MHz, DMSO-d_6)/δ (ppm): 176.8, 164.2, 155.4, 152.8, 147.5, 137.2, 132.3, 131.0, 130.5, 128.9, 125.5, 116.0, 113.0, 103.1. ESI-MS (m/z): 351.2 $[M + H]^+$. HPLC purity = 95.55%, Rt 24.80min.

(E)-5-hydroxy-2-(2-(6-methoxybenzo[d]oxazol-2-yl)vinyl)-4H-pyran-4-one (**9j**). Yellow solid, yield 86.2%. ^{1}H NMR(500 MHz, CD_3Cl,CD_3OD)/δ (ppm)：8.01 (s, 1H, *H-6*), 7.61 (d, 1H, *J* = 8.5 Hz, *H*-4′), 7.42 (d, 1H, *J* = 16.0 Hz, CH=C*H*$_a$), 7.31 (d, 1H, *J* = 16.0 Hz, C*H*$_b$=CH), 7.19 (d, 1H, *J* =2.5 Hz, *H*-7′), 7.03 (dd, 1H, J_1 = 9.0 Hz, J_2 = 2.5 Hz,H-5′), 6.67 (s, 1H, *H*-3), 3.90 (s, 3H, OCH_3). ESI-MS (m/z): 285.2$[M + H]^+$. HPLC purity = 98.74%, Rt 15.08min.

(E)-5-hydroxy-2-(2-(6-methoxy-1-methyl-1H-benzo[d]imidazol-2-yl)vinyl)-4H-pyran-4-one (9**l**). Yellow solid, yield 76.2%. ^{1}H NMR(500 MHz, CD_3OD)/δ (ppm)：7.95 (s, 1H, *H-6*), 7.50 (d, 1H, *J* = 16.0 Hz, CH=C*H*$_a$), 7.44 (d, 1H, *J* = 8.5 Hz, *H*-4′), 7.28 (d, 1H, *J* = 15.5 Hz, C*H*$_b$=CH), 6.96 (d, 1H, *J* =1.5 Hz, *H*-7′), 6.86 (dd, 1H, J_1 = 9.0 Hz, J_2 = 2.0 Hz,H-5′), 6.57 (s, 1H, *H*-3), 3.85 (s, 3H, OCH_3), 3.80 (s, 3H, NCH_3). ESI-MS (m/z): 299.1 $[M + H]^+$. HPLC purity = 96.88%, Rt 32.05min.

(E)-5-hydroxy-2-(2-(6-hydroxybenzo[d]thiazol-2-yl)vinyl)-4H-pyran-4-one (**9i**)

To a solution of compound **9g (**303 mg, 1.0 mmol) in CH_2Cl_2 (10 mL) was added 5mL BBr_3/CH_2Cl_2 solution (1mol/L) in drop wise under ice-water bath. The mixture was stirred for 30 mins and quenched with 5mL cooled methanol. The solvent was removed under reduced pressure and the residue was purified with silica gel chromatoghaphy to afford **9i.** White solid, 61.4% yield. ^{1}H NMR (400 MHz , DMSO-d_6)/δ (ppm): 10.0 (s, 1H, O*H*), 9.32 (s, 1H, O*H*), 8.10 (s, 1H, *H*-6), 7.85 (d, 1H, *J* = 8.8 Hz, *H*-4′), 7.54 (d, 1H, *J* = 16.0 Hz, CH=C*H*$_a$), 7.41 (s, 1H, H-7′), 7.33 (d, 1H, *J* = 16.0 Hz, C*H*$_b$=CH), 7.02 (d, 1H , *J* = 8.0 Hz, H-5′), 6.76 (s, 1H, H-3). ^{13}C NMR (100 MHz, DMSO)/δ (ppm): 174.3, 160.7, 159.6, 157.0, 157.0, 147.4, 139.9, 136.9, 127.7, 124.3, 117.2, 114.5, 107.1. ESI-MS (m/z): 288.3 $[M + H]^+$. HPLC purity = 97.15%, Rt 12.69min.

(E)-5-hydroxy-2-(2-(6-hydroxybenzo[d]oxazol-2-yl)vinyl)-4H-pyran-4-one (**9k**). The same procedure as described for **9i** was used with **9j** to yield **9k** as a Yellow solid, yield 84.2%. ^{1}H NMR(500 MHz, DMSO-d_6)/δ (ppm)：10.12 (s, 1H, O*H*), 9 .43 (s, 1H, *OH*), 8.10 (s, 1H, *H*-6), 7.59 (d, 1H, *J* = 16.0 Hz, CH=C*H*$_a$), 7.46 (d, 1H, *J* = 16.0 Hz, C*H*$_b$=CH), 7.05 (s, 1H, *H*-7′), 6.89 (d, 1H, *J* = 8.0 Hz, H-5′), 6.82 (s, 1H, *H*-3). ^{13}C NMR (125 MHz, DMSO-d_6)/δ (ppm): 175.3, 164.6, 157.1, 155.1, 137.6, 124.2, 120.4, 120.2, 116.1, 108.9, 103.8, 102.4, 100.3, 91.2 .ESI-MS (m/z): 272.0 $[M + H]^+$. HPLC purity = 98.48%, Rt 11.66min.

(E)-5-hydroxy-2-(2-(6-hydroxy-1-methyl-1H-benzo[d]imidazol-2-yl) vinyl)-4H-pyran-4-one(**9m**) The same procedure as described for **9i** was used with **9l** to yield **9m** as a Yellow solid 72.0%. ^{1}H NMR(500 MHz, CD_3OD)/δ (ppm)： 7.71 (s, 1H, *H-6*), 7.27 (d, 1H, *J* = 16.0 Hz, CH=C*H*$_a$), 7.23 (d, 1H, *J* = 9.0 Hz, *H*-4′), 7.12 (d, 1H, *J* = 16.0 Hz, C*H*$_b$=CH), 6.78~6.75 (m, 2H, *H*-5′, *H*-7′), 6.37 (s, 1H, *H*-3), 3.67 (s, 3H, NCH_3). ^{13}C NMR (125 MHz, CD_3OD)/δ (ppm):163.9, 163.0, 152.5, 150.3, 145.4, 140.0, 137.6, 134.8, 133.7, 129.6, 123.3, 119.7, 119.5, 101.9, 95.9, 36.0 . ESI-MS (m/z): 285.1 $[M + H]^+$. HPLC purity = 99.39%, Rt 6.91min.

2-(hydroxymethyl)-5-((4-methoxybenzyl)oxy)-1-methylpyridin-4(1H)-one (**14**)

The mixture of compound **11a** (3.0 g, 11.5 mmol), H_2O (138 mL) and 30% aqueous methylamine (36 mL) was refluxed for 4h. After cooling to room temperature, the mixture was extracted with CH_2Cl_2 (30 mL×3). The combined extract was washed with saturated saline, dried over anhydrous sodium sulfate, and concentrated under reduced pressure to afford **14** as a yellow solid, yield 93%. ^{1}H NMR (500 MHz, DMSO-d_6)/δ (ppm): 7.51 (s, 1H, *H*-6), 7.33 (d, 2H, *J* = 9.0 Hz, *H*-2′, *H*-6′), 6.93 (d, 2H, *J* = 8.5 Hz, *H*-3′, *H*-5′), 6.20 (s, 1H, *H*-3), 5.53 (t, 1H, *J* = 6.0 Hz, O*H*), 4.90 (s, 2H, Ph-C*H*$_2$), 4.36 (d, 2H, *J* = 5.5 Hz, C*H*$_2$OH), 3.75 (s, 3H, OC*H*$_3$), 3.57 (s, 3H, N-C*H*$_3$). ESI-MS (m/z): 276.3 $[M + H]^+$.

5-((4-methoxybenzyl)oxy)-1-methyl-4-oxo-1,4-dihydropyridine-2-carbaldehyde (**15**)

Compound **15** was prepared according to the general procedure for synthesis compound **12a** and **12b**. Yellow solid, yield 44.3%. ^{1}H NMR (500 MHz, DMSO-d_6) /δ (ppm): 9.75 (s,1H, C*H*O), 7.71 (s, 1H, *H*-6), 7.36 (d, 2H, *J* = 8.5 Hz, *H*-2′, *H*-6′), 6.95 (d, 2H, *J* = 8.5 Hz, *H*-3′, *H*-5′), 6.81 (s, 1H, *H*-3), 4.98 (s, 2H, Ph-C*H*$_2$), 3.89 (s, 3H, OC*H*$_3$), 3.76 (s, 3H, N-C*H*$_3$). ESI-MS (m/z): 274.3 $[M + H]^+$.

General procedure for the preparation of 17a and 17b.

The mixture of 2-bromomethyl-benzothiazole (**16a**) (500 mg, 2.19 mmol) with $P(OEt)_3$ (0.86 mL) was refluxed over night. The excess $P(OEt)_3$ was removed under reduced pressure and the residue was purified by silica gel column chromatography to afford **17a**. Yellow oil, yield 98%. Diethyl (benzo[d]thiazol-2-ylmethyl) phosphonate (**17a**). ^{1}H NMR (500 MHz, $CDCl_3$) /δ (ppm): 7.92 (d, 1H, *J* = 8.0 Hz, *H*-3), 7.77 (d, 1H, *J* = 8.0 Hz, *H*-7), 7.39 (t, 1H, *J* = 8.0 Hz, *H*-4), 7.30 (t, 1H, *J* = 7.5 Hz, *H*-6), 4.10-4.05 (m, 4H, 2×C*H*$_2$CH$_3$), 3.67 (d, 2H, *J* = 21.5 Hz, C*H*$_2$P=O), 1.24 (t, 6H, *J* = 7.5 Hz, 2×CH$_2$C*H*$_3$). ESI-MS (m/z): 286.2 $[M + H]^+$.

Diethyl (benzo[d]oxazol-2-ylmethyl)phosphonate (**17b**) Light yellow oil, yield 92.0%. ^{1}H NMR (500 MHz, $CDCl_3$)/δ (ppm): 7.63-7.60 (m, 1H, *H*-3), 7.45-7.43 (m, 1H, *H*-7), 7.27-7.25 (m, 2H, *H*-5, *H*-6), 4.13-4.09 (m, 4H, 2×C*H*$_2$CH$_3$), 3.52 (d, 2H, *J* = 21.5 Hz, C*H*$_2$P=O), 1.26 (t, 6H, *J* = 7.5 Hz, 2×CH$_2$C*H*$_3$). ESI-MS (m/z): 269.2 $[M + H]^+$.

General procedure for the preparation of 18a and 18b.

RSC Advances Accepted Manuscript

This journal is © The Royal Society of Chemistry 20xx

To a soulution of compound **17a** (200.0 mg, 0.71 mmol) in 3 mL anhydrous THF was added sodium hydride (34.1 mg, 1.42 mmol) in small portions under ice-water bath. After stirring for additional 10 min at room temperature, compound **15** (194.0 mg, 0.71 mmol) in anhydrous THF (3 mL) was added in drop wise. The mixture was stirred overnight at room temperature and quenched with water (5 mL), the product precipitated as a yellow solid (172.0 mg, 60.0%). (E)-2-(2-(benzo[d]thiazol-2-yl)vinyl)-5- ((4-methoxybenzyl)oxy)-1-methylpyridin-4(1H)-one (**18a**). ^{1}H NMR (500 MHz, $CDCl_3$)/δ (ppm): 8.16 (d, 1H, *J* = 8.0 Hz, *H*-4'), 8.06 (d, 1H, *J* = 8.0 Hz, *H*-7'), 7.70 (s, 1H, *H*-6), 7.66 (d, 1H, *J* = 16.0 Hz, CH=CH_a), 7.62 (d, 1H, *J* = 16.0 Hz, CH_b=CH), 7.58-7.55 (m, 1H, *H*-5'), 7.51-7.48 (m, 1H, *H*-6'), 7.37 (d, 2H, *J* = 8.5 Hz, *H*-2'', *H*-6''), 6.96 (d, 2H, *J* = 8.5 Hz, *H*-3'', *H*-5''), 6.71 (s, 1H, *H*-3), 4.96 (s, 2H, Ph-CH_2), 3.78 (s, 3H, OCH_3), 3.76 (s, 3H, NCH_3). ESI-MS (m/z): 405.5 $[M + H]^+$.

(E)-2-(2-(benzo[d]oxazol-2-yl)vinyl)-5-((4-methoxybenzyl)oxy)-1-methylpyridin-4(1H)-one (**18b**). Light yellow solid, yield 54.0%. ^{1}H NMR (500 MHz, $CDCl_3$)/δ (ppm): 7.73 (d, 1H, *J* = 8.5 Hz, *H*-4'), 7.56 (d, 1H, *J* = 15.0 Hz, CH=CH_a), 7.51 (d, 1H, *J* = 6.5 Hz, *H*-7'), 7.38-7.30 (m, 4H, *H*-5', *H*-6', *H*-2'', *H*-6''), 7.04（d, 1H, *J* = 15.6 Hz, CH_b=CH), 6.94（s, 1H, *H*-6), 6.86（d, 2H, *J* = 10.0 Hz, *H*-3'', *H*-5''), 6.77 (s, 1H, *H*-3）, 5.13（s, 2H, Ph-CH_2), 3.77 (s, 3H, OCH_3), 3.63 (s, 3H, NCH_3). ESI-MS (m/z): 389.4 $[M + H]^+$.

General procedure for the preparation of 9n and 9o.

The mixture of compound **18a** (101 mg, 0.25 mmol) with 5mL CF_3COOH/CH_2Cl_2 (1:1) was stirred for 1h at room temperature. After removal of solvent under reduced pressure, the residue was purified with silica gel chromatoghaphy to get **9n** as white solid, yield 91.2%. (E)-2-(2-(benzo[d]thiazol-2-yl)-vinyl)- 5-hydroxy-1-methylpyridin-4(1H)-one. ^{1}H NMR (400 MHz, $CDCl_3/CD_3OD$)/δ (ppm): 8.17 (s, 1H, *H*-6), 8.05 (d, 1H, *J* = 8.0 Hz , *H*-4'), 7.99 (d, 1H, *J* = 8.0 Hz, *H*-7'), 7.82 (d, 1H, *J* = 15.6 Hz, CH=CH_a), 7.71 (d, 1H, *J* = 15.6 Hz, CH_b=CH), 7.59-7.48 (m, 3H, *H*-5', *H*-6', *H*-3), 4.20 (s, 3H, CH_3). ^{13}C NMR (100 MHz, $CDCl_3/CD_3OD$)/δ (ppm): 163.6, 159.9, 151.7, 145.7, 143.6, 134.5, 131.9, 130.3, 127.1, 126.5, 124.3, 122.4, 121.8, 110.7, 43.9. ESI-MS (m/z): 285.4 $[M + H]^+$. HPLC purity = 99.01%, Rt 17.33min.

(E)-2-(2-(benzo[d]oxazol-2-yl)vinyl)-5-hydroxy-1-methylpyridin-4(1H)-one (**9o**). Yellow solid, 74.6% yield. ^{1}H NMR (400 MHz , DMSO-d_6) /δ(ppm): 8.29 (s, 1H, *H*-6), 7.90 (d, 1H, *J* = 16.0 Hz , CH=CH_a), 7.85 (d, 1H, *J* = 7.6 Hz, *H*-4'), 7.81 (d, 1H, *J* = 8.0 Hz, *H*-7'), 7.67 (s, 1H, *H*-3), 7.57 (d, 1H, *J* = 15.6 Hz, CH_b=CH), 7.53-7.44 (m, 2H, *H*-5', *H*-6'), 4.18 (s, 3H, CH_3). ^{13}C NMR (100 MHz, DMSO-d_6) /δ (ppm): 161.0, 160.4, 150.4, 145.8, 143.6, 141.8, 133.2, 128.5, 127.2, 125.8, 123.4, 120.8, 112.0, 111.4, 44.5. ESI-MS (m/z): 269.5 $[M + H]^+$. HPLC purity = 99.57%, Rt 9.09min.

HL_5 and **HL_{12}** was prepared according to the references.[32,33]

HL_5 ^{1}H NMR (500 MHz , $CD_3OD/CDCl_3$) /δ(ppm):8.45 (d, 1H, *J* = 7.0, *H*-6), 8.17 (t, 2H, *J* = 7.5, *H*-4', *H*-7'), 7.74 (t, 1H, *J* = 8.0, *H*-5'), 7.69 (t, 1H, *J* = 7.5, *H*-6'), 7.36 (d, 1H, *J* = 6.0, *H*-5), 2.58 (s, 3H, CH_3).^{13}C NMR (125 MHz , $CD_3OD/CDCl_3$) /δ(ppm):162.3, 157.3, 149.2, 144.2, 141.8, 138.3, 135.6, 127.9, 127.8, 124.4, 122.4, 111.0, 13.8. ESI-MS (m/z): 245.1 $[M + H]^+$.

HL_{12} ^{1}H NMR (500 MHz , $CD_3OD/CDCl_3$) /δ(ppm): 7.80 (d, 1H, *J* = 8.0, *H*-6), 7.95 (d, 1H, *J* = 8.0, *H*-4'), 7.79 (d, 1H, *J* = 7.0, *H*-7'), 7.55 (t, 1H, *J* = 8.0, *H*-5'), 7.52 (t, 1H, *J* = 8.0, *H*-6'), 6.52 (d, 1H, *J* = 7.0, *H*-5), 5.68 (s, 2H, CH_2), 2.43 (s, 3H, CH_3). ^{13}C NMR (125 MHz , $CD_3OD/CDCl_3$) /δ(ppm):170.0, 165.7, 152.7, 146.1, 138.4, 134.8, 131.4, 126.6, 125.9, 123.0, 121.8, 112.0, 55.1, 11.5. ESI-MS (m/z): 273.1 $[M + H]^+$.

ACKNOWLEDGEMENTS

The authors thank the National Natural Science Foundation of China (No.21172193), Zhejiang Provincial Natural Foundation of China (No.R2110297) for financial support. We also thank Jianyang Pan (Pharmaceutical Informatics Institute, Zhejiang University) for performing NMR and MS for structure elucidation.

Reference

1. V. H. Finder, *J. Alzheimers Dis.* ,2010, **22** Suppl 3, 5-19.
2. C. Lu, Y. Guo, J. Yan , Z. Luo, H. B. Luo, M. Yan, L. Huang and X. Li, *J. Med. Chem.*, 2013, **56**, 5843-5859.
3. G. Pepeu and M. G. Giovannini, *Curr. Alzheimer Res.*,2009, **6**, 86-96.
4. R. Bullock, *Alzheimer Dis. Assoc. Disord.*, 2006, **20**, 23-29.
5. A. Cavalli, M. L. Bolognesi, A. Minarini, M. Rosini, V. Tumiatti, M. Recanatini and C. Melchiorre, *J. Med. Chem*., 2008, **51**, 347-372.
6. A. Alzheimer's, *Alzheimers. Dement.*, 2013, **9**, 208-245.
7. C. Ballard, S. Gauthier, A. Corbett, C. Brayne, D. Aarsland, E. Jones, *Alzheimer's disease. Lancet* .,2011, **377**, 1019-1031.
8. J. D. Grill, J. L. Cummings, *Expert Rev. Neurother.*, 2010, **10**, 711-728.
9. R. Anand, K. D. Gill, A. A. Mahdi, *Neuropharmacology*., 2014, **76**, 27-50.
10. K. Chiang, E. H. Koo, *Annu. Rev. Pharmacol Toxicol*., 2014, **54**, 381-405.
11. G. Pepeu, M. G. Giovannini, *Curr. Alzheimer Res*., 2009, **6**,86–96.
12. A. S. Pithadia, M. H. Lim, *Current Opinion in Chemical Biology*., 2012, **16**, 67-73.
13. R. Jakob-Roetne, H. Jacobsen, *Angewandte Chemie, International Edition*., 2009, **48**, 3030-3059.
14. A. G. William, J. H. ndez-Guzmán, W. K. Jesse, L. Sun, A. S. Veronika and K. Warncke. *J. Am. Chem. Soc.*, 2012, **134**, 18330−18337.
15. P. Faller. *ChemBioChem*., 2009, **10**, 2837–2845.
16. P. Faller and C. Hureau. *Dalton Trans.*, 2009, 1080–1094.
17. J. A. Duce, A. Tsatsanis, M. A. Cater, S. A. James, E. Robb, K. Wikhe, S. L. Leong, K. Perez, T. Johanssen, M. A. Greenough, H. H. Cho, D. Galatis, R. D. Moir, C. L. Masters, C. McLean, R. E. Tanzi, R. Cappai, K. J. Barnham, G. D. Ciccotosto, J. T. Rogers, A. I. Bush, *Cell,* 2010, **142**, 857-867.
18. X. Huang, C. S. Atwood, M. A. Hartshorn, G. Multhaup, L. E. Goldstein, R. C. Scarpa, M. P. Cuajungco, D. N. Gray, J. Lim, R. D. Moir, R. E. Tanzi, A. I. Bush, *Biochemistry*, 1999, **38**, 7609−7616.
19. R. Leon, A. G. Garcia and M. Contelles, *J. Med. Res. Rev*., 2013, **33**, 139-189.
20. J. A. Hardy, G. Higgins, *Science*, 1992, **256**, 184-185.
21. C. C. Glabe, *Subcell. Biochem*., 2005, **38**, 167−177.
22. J. Hardy, D. J. Selkoe, *Science,* 2002, **297**, 353-356.
23. E. Karran, M. Mercken and B. De Strooper, *Nat. Rev. Drug Discovery*, 2011, **10**, 698−712.
24. H. Amijee and D. I. Scopes, *J. Alzheimer's Dis.,* 2009, **17**, 33–47.
25. L. S. Wolfe, M. F. Calabrese, A. Nath, D. V. Blaho, A. D. Miranker and Y. Xiong, *Proc. Natl. Acad. Sci. U S A*, 2010, **107**, 16863-16868.
26. M. Biancalana, K. Makabe, A. Koide and S. Koide, *J. Mol. Biol*., 2009, **385**, 1052-1063
27. J. O. Rinne, D. F. Wong, D.A. Wolk, V. Leinonen, S. E. Arnold, C. Buckley, A. Smith, R. McLain, P. F. Sherwin, G. Farrar, M. Kailajarvi, I.D. Grachev, *Acta Neuropathol*., 2012, **124**, 833–845.
28. H. F. Kung, S. R. Choi, W. Qu, W. Zhang, D. Skovronsky, *J. Med. Chem*., 2010, **53**, 933-941.
29. C. Lu, Y. Guo, J. Li, M. Yao, Q. Liao, Z. Xie and X. Li, *Bioorg. Med. Chem. Lett.,* 2012, **22**, 7683−7687.
30. K. Ono, Y. Yoshiike, A. Takashima, K. Hasegawa, H. Naiki and M. Yamada, *J. Neurochem.,* 2003, **87**, 172−181.
31. C. Lu, Y. Guo, J. Yan, Z. Luo, H. B. Luo, M. Yan, L. Huang, X. Li, *J. Med. Chem.,* 2013, **56**, 5843-5859.
32. M. A. Telpoukhovskaia, C. Rodrıguez-Rodrıguez, J. F. Cawthray, L. E. Scott, B. D. G. Page, J. A. Torres, M. Sodupe, G. A. Bailey, B. O. Patricka, C. Orvig, *Metallomics,* 2014, **6**, 249-262
33. L. E. Scott, C. Rodrıguez-Rodrıguez, M. Merkel, M. L. Bowen, D. G. Brent, D. E.Green, T. Storr, F. Thomas, D. A. David, P. R. Lockman, B. O. Patrick, M. J. Adamd and C. Orvig, *Chem. Sci.*, 2011, **2**, 642-648.
34. L. E. Scott, B. D. Page, B. O. Patrick, C. Orvig, *Dalton Trans.,* 2008, **45**, 6364-6367.
35. D. E. Green, M. L. Bowen, L. E. Scott, T. Storr, M. Merkel, K. Bohmerle, K. H. Thompson, B. O. Patrick, H. J. Schugar, C. Orvig, *Dalton Trans.,* 2010, **39**, 1604-1615.
36. M. A. Telpoukhovskaia, B. O. Patrick, C. Rodriguez-Rodriguez and C. Orvig, *Mol Biosyst.,* 2013 , **9**, 792-805.

RSC Advances Accepted Manuscript

37. L. Tang, L. Zhao, L. Hong, F. Yang, R. Sheng, J. Chen, Y. Shi, N. Zhou, Y. Hu, *Bioorg. Med. Chem.*, 2013, **21**, 5936-5944.
38. R. Sheng, L. Tang, L. Jiang, L. Hong, Y. Shi, N. Zhou, Y. Hu. Novel 1-phenyl-3-hydroxy-4-pyridinone derivatives as Multifunctional Agents for the therapy of Alzheimer's Disease. *ACS chemical neuroscience*, in press.
39. B. D. Liboiron, K. H. Thompson, G. R. Hanson, E. Lam, N. Aebischer and C. Orvig, *J. Am. Chem. Soc.,* 2005, **127**, 5104-5115.
40. O. Crescenzi, S. Tomaselli, R. Guerrini, S. Salvadori, A. M. D'Ursi, P. A. Temussi, D. Picone, *Eur. J. Biochem.,* 2002, **269**, 5642-5648.
41. K. Anuj, S. T. Sharma, J. K. Pavlova, F. Darren, J. H. Nicholas, P. R. Nigam, K. Jungsu, M. M. Liviu, *J. Am. Chem. Soc.*, 2012, **134**, 6625−6636.
42. V. Tõugu, A. Karafin, K. Zovo, R. S. Chung, C. Howells, A. K. West, P. Palumaa, *J. Neurochem.*, 2009, **110**, 1784-1795.

RSC Advances Accepted Manuscript

This journal is © The Royal Society of Chemistry 20xx

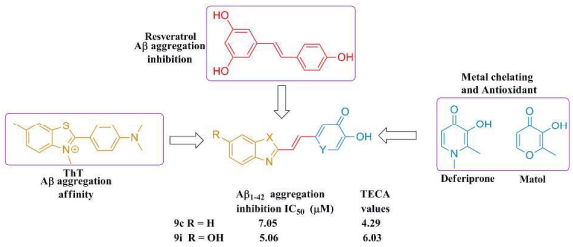

A series of 2-subsituted benzothiazole derivatives were designed and synthesized as MDTLs for potential AD therapy.

RSC Advances Accepted Manuscript